Electrochimica Acta 476 (2024) 143710

Contents lists available at ScienceDirect

Electrochimica Acta

journal homepage: www.journals.elsevier.com/electrochimica-acta

Photoelectrocatalytic chemical oxygen demand analysis using a TiO_2 nanotube array photoanode

Patricia García-Ramírez [a,b], Carlos Antonio Pineda-Arellano [c], Daysi Elusaí Millán-Ocampo [d], Alberto Álvarez-Gallegos [d], Ignasi Sirés [e,*], Susana Silva-Martínez [d,*]

[a] Posgrado en Ingeniería y Ciencias Aplicadas, Centro de Investigación en Ingeniería y Ciencias Aplicadas, Universidad Autónoma del Estado de Morelos, Av. Universidad 1001. Col. Chamilpa, C.P. 62209 Cuernavaca, Morelos, Mexico
[b] CONAHCYT – Centro de Investigaciones en Óptica, A.C. 1-948, C.P. 37000, Lomas del Bosque 115, Col. Lomas del Campestre, C.P. 37150, León, Guanajuato, Mexico
[c] CONAHCYT-Centro de Investigaciones en Óptica A.C. Prol. Constitución 607, Fracc. Reserva Loma Bonita. Código Postal 20200, Aguascalientes, Aguascalientes, Mexico
[d] Centro de Investigación en Ingeniería y Ciencias Aplicadas, Universidad Autónoma del Estado de Morelos, Av. Universidad 1001, Col. Chamilpa, C.P. 62209, Cuernavaca, Morelos, Mexico
[e] Laboratori d'Electroquímica dels Materials i del Medi Ambient, Departament de Ciència de Materials i Química Física, Secció de Química Física, Facultat de Química, Universitat de Barcelona, Martí i Franquès 1-11, 08028 Barcelona, Spain

ARTICLE INFO

Keywords:
COD analysis
Photoanode
Photocatalysis
Photoelectrocatalysis
TiO_2 nanotubes

ABSTRACT

The chemical oxygen demand (COD) is a widely used parameter to evaluate the quality of water for industrial applications. Currently, the standardized method for COD analysis employs expensive and harmful reagents that require a special treatment for disposal upon use. The photoelectrocatalytic COD detection, based on the photocatalytic activity of a reduced TiO_2 nanotube array photoanode (Ti|NT-TiO_2) under supply of a low bias potential, represents a fast, cheap and eco-friendly alternative to the standard COD method (COD_{STD}). Here, Ti|NT-TiO_2 was synthesized by the anodization method followed by heat treatment and electrochemical reduction. Potassium hydrogen phthalate, glucose and acetic acid were used as model organic compounds. The photoelectrocatalytic detection of COD (COD_{PEC}) is based on the photoelectrocatalytic oxidation of target compounds on the surface of the reduced Ti|NT-TiO_2 under UV illumination. Photocurrent transients were recorded using chronocoulometry, and the net charge (Δq) was plotted as a function of the theoretical COD (COD_{TH}). A linear relationship was found between these two parameters regardless of the model compound. That relationship was used to determine the COD_{PEC} for acetylsalicylic acid and Terasil Blue dye solutions at concentrations within the range of 0–15 mg L^{-1}. A good agreement between COD_{PEC} and COD_{STD} was achieved. The limit of detection of the method was 3.6 mg L^{-1} COD, with the linear range established from 0 to 50 mg L^{-1}.

1. Introduction

The global population reached 8.0 billion in mid-November 2022, and it is expected to increase in the next years. This will entail a much higher energy demand to produce all the necessary goods, with the simultaneous need of advanced technology for treating a large volume of wastewater and monitoring the quality of regenerated water. As part of one of the most polluting sectors, textile companies have negative impacts on the environment and health due to the potential hazard of synthetic dyes and their reaction by-products.

The level of pollution caused by organic compounds present in water bodies can be measured by a varied set of techniques [1,2], such as total organic carbon (TOC), biological oxygen demand (BOD), and chemical oxygen demand (COD) analysis, which are ubiquitously employed to assess general water quality [3]. Some disadvantages of BOD analysis include the long time needed, the difficulty to be standardized, and its poor precision and reproducibility [4]. On the other hand, the most reliable TOC analyzers are expensive and usually non-portable [5,6]. COD determination involves the measurement of the amount of oxygen consumed during organic matter oxidation reaction using a strong oxidant in acidic solution [7,8]. COD is most typically determined through a standardized method, which has a few disadvantages that limit its wider application: strong chemical oxidants like potassium permanganate ($KMnO_4$) or potassium dichromate ($K_2Cr_2O_7$), along with

* Corresponding authors
E-mail addresses: i.sires@ub.edu (I. Sirés), ssilva@uaem.mx (S. Silva-Martínez).

https://doi.org/10.1016/j.electacta.2023.143710
Received 4 October 2023; Received in revised form 11 December 2023; Accepted 16 December 2023
Available online 29 December 2023

corrosive (H_2SO_4), expensive (Ag) and toxic (Hg) chemical reagents, are required. Moreover, a long reflux time is needed, and detection sensitivity is rather low [9–11]. To address these problems, several research groups have proposed alternative methods that are cheaper, faster, easier to operate and environmentally friendly. The determination of COD by electrochemical techniques, which are based on the use of electrodes with high catalytic activity, rapid response and cost-effectiveness [12], has been established to provide an alternative to the standardized method. Several catalytic working electrodes based on carbon [12], boron-doped diamond [13,14], cobalt oxide [15], copper [10,16], nickel [17], Pt modified with PbO_2 [18] and Al/SnO_2-TiO_2 [19] have been successfully used for this purpose. TiO_2 is also an ideal candidate for this application at industrial scale due to its chemical stability, non-toxicity, wide bandgap, high catalytic activity, easy synthesis, and low cost [20–22]. Nevertheless, TiO_2 undergoes a fast electron-hole pair recombination. Therefore, several scholars have tried to minimize the charge carrier recombination by: (i) Modifying the bandgap through doping with metals [23–26]; (ii) applying a bias potential to the supported photocatalyst, operating under the so-called photoelectrocatalytic (PEC) conditions [24,27]; and (iii) through electrochemical partial reduction of Ti^{4+} to Ti^{3+} [28], among other strategies. This might eventually bring about a faster, more efficient and accurate alternative to conventional analysis [29].

Following these concepts, COD analysis has been carried out by employing different TiO_2 nanostructures, such as highly-ordered titania nanotube arrays [30,31], Cu_2O-loaded titania nanotube arrays [32], chalcogenide Te/TiO_2/Ti nanotube arrays [33], titania nanorod arrays [34], TiO_2 nanoporous electrodes [3] and TiO_2 nanoparticle film electrodes [35]. For example, Zhang et al. [3] used a reduced TiO_2 nanoporous electrode as a sensor for the determination of COD by PEC method with a bias potential of +1.5 V (vs Ag/AgCl reference electrode). They reported a considerable improvement in PEC activity, which can be attributed to the nanoporous structure, the increase in Ti(II)/Ti (III)/oxygen vacancies, and a significant improvement in donor density [36]. The PEC determination of COD using TiO_2 nanotube arrays using a thin-cell reactor was reported as well [30,31]. Zheng et al. [30] compared the COD performance of a TiO_2 nanotube array and a coated TiO_2 nanofilm, reporting a higher photoactivity with the former; in addition, a proportional relationship between the net charge and the COD value obtained by the standard method was reported. Zhang et al. [31] examined different parameters (i.e., Cl^- and NH_4^+ concentration, anodic potential, anodic time, solution pH, calcination temperature) that have influence on the performance of the PEC determination. That study showed a strong decrease in the COD value obtained using a TiO_2 nanotube array sensor when the solution pH was below 4 or above 10, and at chloride ion concentration above 2500 mg L^{-1}. Moreover, Cu_2O-loaded titania nanotube arrays [32] were employed for the determination of COD under visible light. The photocurrent response of this composite was higher than that observed for pristine TiO_2 nanotube array under visible light. A COD detection limit of 15 mg L^{-1} was reported within a COD range between 20-300 mg L^{-1}; the authors found the anodic photocorrosion of Cu_2O-loaded TiO_2 nanotube arrays. Nurdin et al. [33] studied the effect of Te doping on TiO_2/Ti nanotube arrays, finding an improvement of the PEC properties. This was attributed to a decrease in the recombination of electron-hole pairs during photoactivation, promoting a massive surface reaction with organic compounds and improving the detection sensitivity. Titania nanorod arrays [34] and TiO_2 nanoparticle film electrodes [35] have also been synthetized to generate COD sensors. Using the former material, Wang et al. studied the effects of parameters such as applied potential, light intensity and pH, reporting that the pH range suitable for the COD determination was between pH 4 and 10. Additionally, the COD determination method showed a limit of detection (LOD) of 18.3 mg L^{-1} and a linear range between 20–280 mg L^{-1}. Finally, Zhao and collaborators [35] reported that their PEC method was sensitive and capable of detecting a COD as low as 0.2 mg L^{-1}.

Considering all these studies, herein, the photoelectrocatalytic detection of COD (COD_{PEC}), based on the photoelectrocatalytic activity of reduced Ti|TiO_2 nanotube array (i.e., Ti|NT-TiO_2) photoanode with supply of a low bias potential is reported. A net charge (Δq), calculated from the area under the chronocoulometric photocurrent vs time curve, was obtained for three model compounds (potassium phthalate monobasic, glucose and acetic acid) with known theoretical COD. The resulting calibration curves served to determine COD_{PEC} from aqueous solutions of acetylsalicylic acid (ASA) and Terasil Blue (TB) textile dye solutions.

2. Materials and methods

2.1. Reagents

Ethylene glycol (98% purity), ammonium fluoride, sodium sulphate, sodium hydroxide, ammonium hydroxide, sulfuric acid, ethanol, acetone, potassium phthalate monobasic (KHP), glucose (G) and acetic acid (AA) were purchased from Sigma-Aldrich and used as received. Acetylsalicylic acid (ASA, 500 mg Aspirin tablets) was purchased from a local pharmacy and a local textile company from Mexico provided Terasil Blue 3RL (TB, $C_{14}H_9BrN_2O_4$) textile dye. Titanium foil (99.6% purity, 0.2 mm thickness) was acquired from Sigma Aldrich. COD_{STD} values were determined using standard reagents and a standard procedure (Hach). All the analytical solutions were prepared with distilled water (J.T. Baker).

2.2. Synthesis of the TiO_2 nanotubes

The synthesis of TiO_2 nanotubes was carried out by conventional anodization in a two-electrode cell (40 mL capacity) containing 0.5 wt.% NH_4F and 10 wt.% water in ethylene glycol. A constant potential difference of 50 V was applied between a titanium foil (2 cm × 1 cm) and a platinum mesh for 60 min to form the TiO_2 nanotube array. The anodized titanium foil was rinsed with distilled water and placed in a 0.1 M NaOH solution for 30 min. Subsequently, it was washed with distilled water, dried at room temperature, and finally annealed at 600 °C for 120 min [37]. After heat treatment, the material was electrochemically reduced, causing the transition from Ti^{4+} to Ti^{3+}, eventually yielding the reduced Ti|TiO_2 nanotube array photoanode (i.e., Ti|NT-TiO_2). The electrochemical reduction was performed in a three-electrode cell using the nanotube array as the anode, a Pt mesh as the counter electrode, and Ag|AgCl as reference electrode, all of them connected to a BASi Epsilon model E2 potentiostat interfaced with a computer to register the current. A negative current (-5 mA) was applied to the working electrode for 10 min in an aqueous electrolyte containing 20 mL of 0.1 M H_2SO_4 at room temperature [3] followed by rinsing with distilled water. A set of Ti|NT-TiO_2 electrodes was synthesized to be used as photoanodes.

2.3. Characterization of Ti|NT-TiO_2

The morphology of Ti|NT-TiO_2 was analysed by scanning electron microscopy (JEOL JSM-6010LA microscope). The crystal structures were evaluated in an X-ray diffractometer (Bruker D2 PHASER, 2nd generation) recording the spectra within the 2θ-range of 20-70° with a grazing incidence angle of 0.5°. The photoelectrochemical characterization of each Ti|NT-TiO_2 photoanode was carried out by means of linear sweep voltammetry. For this, a three-electrode quartz electrochemical cell that contained a 50 mM Na_2SO_4 electrolyte was used. The Ti|NT-TiO_2 photoanode (working electrode), a Pt mesh (counter electrode) and Ag|AgCl (3 M KCl reference electrode) were connected to the aforementioned potentiostat to record the current (in the dark) and photocurrent (under UV illumination) as a function of the applied potential (positive scan from -0.5 V up to 1.0 V vs Ag|AgCl, at a scan rate of 10 mV s^{-1}). The UV light came from a quartz-jacketed mercury Pen-Ray lamp (λ = 254 nm, intensity 2 W cm^{-2}, model 11SC-1, from Analytik

Jena), which was placed in front of the Ti|NT-TiO_2 array photoanode separated 0.5 cm from the electrochemical cell and with a lighting area equivalent to 1 cm^2. All experiments were carried out inside a black box to avoid interference from external lighting.

2.4. Photoelectrocatalytic detection of COD

Photoelectrocatalytic detection of COD (i.e., COD_{PEC}) is based on a non-exhaustive photocatalytic oxidation mode to keep the concentration of the target compound almost constant before and after the photocurrent flow, so that the photocurrent remains stable during that period. Photocurrent transients are recorded upon photocatalytic oxidation of the organic compounds on the surface of Ti|NT-TiO_2, which is fed with a bias potential and exposed to UV illumination from the same lamp mentioned above. Transient photocurrent responses of the Ti|NT-TiO_2 anode were obtained by the chronocoulometric technique using the aforementioned potentiostat and counter and reference electrodes. A three-electrode cell containing 20 mL of aqueous 50 mM Na_2SO_4 solution with or without a target organic compound (such as KHP, G and AA) was used. A positive bias potential (+1.0 V vs Ag/AgCl) was applied to the Ti|NT-TiO_2 electrode for 60 s at room temperature in the absence or presence of target compounds with known theoretical COD (i.e., COD_{TH}). Concentrations of KHP, G and AA within the range 0-70 mg L^{-1} were used. For each tested concentration of each target compound, a net charge ($\Delta q = q_{\text{target compound}} - q_{\text{electrolyte}}$) was obtained from the area under the chronocoulometric photocurrent vs time curve. A calibration curve was then constructed by plotting the Δq values, obtained from tested concentrations of all target compounds, against the known theoretical COD values (i.e., COD_{TH}) corresponding to the different concentrations of each model compound. Said calibration curve was used to obtain the COD_{PEC} of aqueous solutions of ASA and TB at concentrations ranging from 0 to 15 mg L^{-1}. The stock solution of ASA (100 mg L^{-1} in 50 mM Na_2SO_4) was prepared with hot distilled water (70 °C) to dissolve the required concentration of aspirin; when it reached room temperature, Na_2SO_4 was added before diluting the solution to the desired volume. Finally, the stability of the Ti|NT-TiO_2 electrode was tested by recording a linear voltammogram (as shown in Fig. 2) before using the reduced TiO_2 nanotube array electrode to determine COD.

3. Results and discussion

3.1. Characterization of the nanotube array photoanode

Fig. 1 shows the SEM micrograph and the XRD pattern of the Ti|NT-TiO_2 nanotube array after annealing at 600 °C followed by electrochemical reduction. Well-defined and uniformly distributed nanotubes (Fig. 1a), with an internal diameter ranging from 47 to 55 nm, can be observed throughout the whole surface, whereas characteristic Ti and TiO_2 diffraction peaks are identified in the X-ray diffractogram (Fig. 1b). The peaks correspond to anatase phase as the predominant crystal structure of the TiO_2 nanotube array, with minor presence of rutile phase, in good agreement with the selected annealing temperature.

The photoelectrochemical characterization of the photoanodes was carried out by recording transient photocurrent responses from linear sweep voltammetry tests performed in a three-electrode cell configuration under UV illumination, as shown in Fig. 2. The photoanodes (TiO_2 nanotubes obtained after annealing, and Ti|NT-TiO_2 resulting from subsequent electrochemical reduction process) were tested in a solution containing 50 mM Na_2SO_4 at neutral pH. The quartz cell was placed inside an in-house-built black box containing a UV lamp. Transient photocurrent responses were recorded from -0.5 V to 1.0 V at a scan rate of 10 mV s^{-1}. The photocurrent flows upon irradiation with UV light, owing to the generation of photoinduced charge carriers (electrons in the conduction band (e^-_{CB}) and holes in the valence band (h^+_{VB})), with the subsequent generation of hydroxyl radicals ($^{\bullet}OH$) stimulated by the oxidation of H_2O/OH^- by h^+_{VB} [38–40]. Transient saturation photocurrents at potentials above +0.4 V can be observed for the annealed TiO_2 nanotubes and electrochemically-reduced Ti|NT-TiO_2 photoanodes,

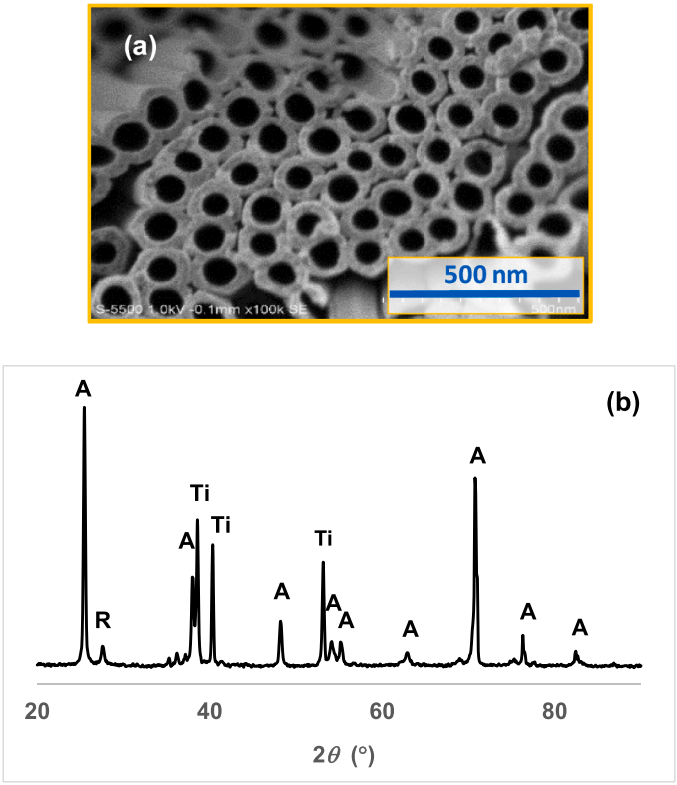

Fig. 1. (a) SEM micrograph and (b) XRD pattern of the synthesized Ti|NT-TiO_2. The materials were subjected to heat treatment at 600 °C (A: anatase; R: rutile; Ti: titanium).

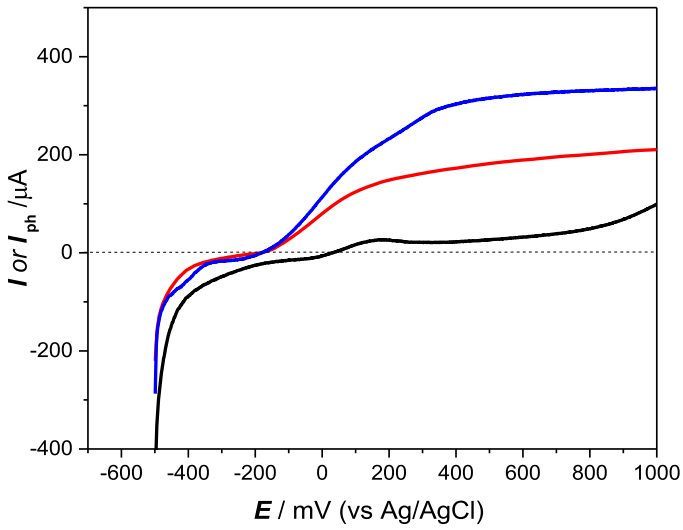

Fig. 2. Linear voltammograms with annealed TiO_2 nanotubes (red curve) and reduced Ti|NT-TiO_2 (blue curve) electrodes under UV illumination, along with Ti|NT-TiO_2 electrode in the dark (black curve). Conditions: 50 mM Na_2SO_4 electrolyte at pH 7, and scan rate of 10 mV s^{-1}.

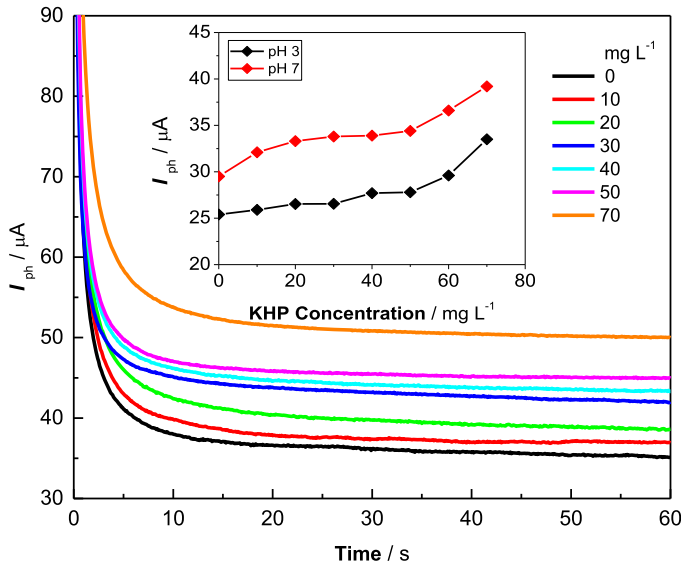

Fig. 3. Photocurrent over time obtained by chronocoulometry for the oxidation of potassium hydrogen phthalate (KHP) as model organic compound at different concentrations in 50 mM Na_2SO_4 with Ti|NT-TiO_2 photoelectrode at pH 7. The inset shows the dependence of photocurrent with KHP concentration at 60 s for each pH value.

with the latter exhibiting higher photocurrent flux. This superiority can be attributed to the partial reduction of Ti^{4+} to Ti^{3+}, which increases the adsorption of water on the TiO_2 surface and the generation of oxygen vacancies that enhance the carrier density, thereby stimulating a better separation efficiency and a higher production of hydroxyl radicals [28]. Note that, in the absence of UV radiation, a low transient current flow between 0.15 V and 0.7 V was obtained, which increases at a potential greater than 0.7 V due to the direct electro-oxidation of water to oxygen.

3.2. Photoelectrocatalytic analysis (PEC) of chemical oxygen demand using a reduced photoanode (Ti|NT-TiO_2)

PEC method quantifies the net electric charge based on the photocurrent transients recorded by the chronocoulometric method from the oxidation of water ($q_{electrolyte}$) and the photocatalytic oxidation of target organic compounds such as KHP, G and AA ($q_{target\ compound}$), using the reduced Ti|NT-TiO_2 photoanode, which is exposed to UV light and fed with a low bias potential (+1.0 V vs Ag/AgCl). According to the literature [41], the electric potential prevents the recombination of h^+/e^- and increases the efficiency of photocatalytic oxidation. In addition, it allows determining the electrons generated during the oxidation reaction and, finally, the concentration of the organic compound in the sample. A sufficiently positive bias potential is needed to ensure the maximum PEC efficiency and, based on the profiles shown in Fig. 2, the photocurrent saturation is found between +0.4 V and +1.0 V. Therefore, the value chosen as bias potential for COD analysis in the samples was +1.0 V.

The net charge transferred during the photoelectrocatalytic degradation of the organic compounds was obtained by the integration of the current-time transients according to the Faraday's law. The photocurrent or net charge corresponds to a direct quantification of the stoichiometric degradation of the organic compounds at the Ti|NT-TiO_2 anode by PEC, according to reactions (1) to (3):

$$\text{KHP}: \ C_8H_5O_4^- + 12H_2O \rightarrow 8CO_2 + 29H^+ + 30e^- \quad (1)$$

$$\text{G}: \ C_6H_{12}O_6 + 6H_2O \rightarrow 6CO_2 + 24H^+ + 24e^- \quad (2)$$

$$\text{AA}: \ C_2H_4O_2 + 2H_2O \rightarrow 2CO_2 + 8H^+ + 8e^- \quad (3)$$

The responses when using KHP as probe are shown in Fig. 3, evidencing a photocurrent increase as the KHP concentration is risen; similar photocurrent transients performed in triplicate were recorded for each concentration of organic compounds G and AA (not shown). Furthermore, the inset of Fig. 3 shows a linear behavior between 0 and 50 mg L^{-1} KHP at pH 3 and pH 7, obtaining higher photocurrents at pH 7. Under neutral conditions, the anode surface is at its point of zero charge (pzc), that is, without a net charge (TiOH) when the pH of the solution is equal to pzc. At pH < pzc, the adsorption sites on the anode surface become positively charged ($TiOH_2^+$) due to proton adsorption and negatively charged (TiO^-) at pH > pzc upon proton desorption. The pzc for TiO_2 has been reported at pH between 6.3 and 7.1 [42–45]. The adsorption sites on the Ti|NT-TiO_2 anode surface, having no net charge, were more favorable for the adsorption of phthalate anion, P^{2-} ($pK_a\left(\frac{HP^-}{P^{2-}}\right) = 5.4$), which justifies its enhanced oxidation at pH 7.

Fig. 4 shows the correlation of the net charges (Δq) of KHP, G and AA at pH 3 and 7 against the concentration of the three target compounds (Fig. 4a), and against their theoretical COD values (COD_{TH}) (Fig. 4b). It can be observed that the charges increase proportionally as the concentrations and theoretical COD of all compounds are enhanced. Moreover, Fig. 4a shows that a steeper curve slope was obtained as the molar mass of the compound became higher, which is consistent with the larger number of electrons involved in reactions (1) to (3) for the degradation of the organic compounds (30, 24 and 8 e^- for KHP, G and AA, respectively). Furthermore, higher net charges and slope values were obtained at pH 7, as depicted in Fig. 4a. Based on the ionization (acidity) constants (K_a) of KHP, G and AA, and the mole fraction distribution as a function of pH, at pH 7, there is 97.5 % phthalate anion, P^{2-} ($pK_a\left(\frac{HP^-}{P^{2-}}\right) = 5.4$), 99.4 % acetate anion, Ac^- ($pK_a\left(\frac{HAc}{Ac^-}\right) = 4.75$), and 100% glucose, G (first $pK_a\left(\frac{G}{G^-}\right) = 12.18$). Therefore, the absence of electrostatic repulsion between the P^{2-}, Ac^-, or G species, with negative or zero charge, and the zero charge adsorption sites on the anode surface facilitated the oxidation of these species due to better adsorption. The K_a and type of compounds (Table 1) is thus a relevant parameter that informs about the chemical nature of the molecules with acid-base properties. This can determine their tendency to become oxidized, producing structural changes in the molecules upon UV irradiation and applied bias potential.

Moreover, the recorded photocurrents for each target compound are virtually independent of their structure when photoelectrocatalytically oxidized under similar conditions, as shown in Fig. 4b. This figure shows

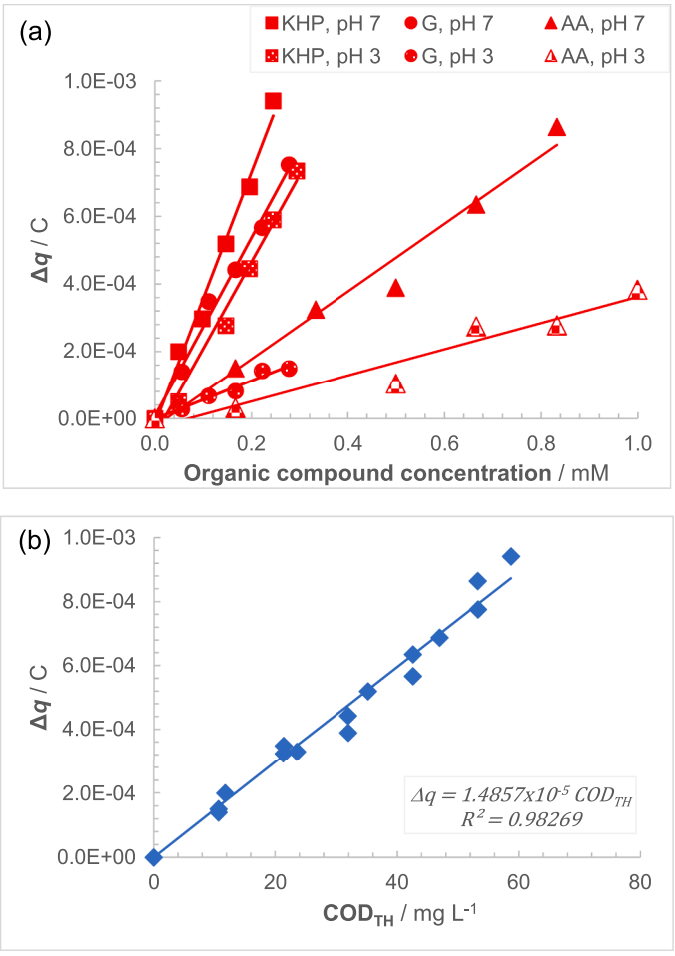

Fig. 4. Correlation between Δq and: (a) concentration of target compounds (AA: acetic acid; G: glucose; KHP: potassium hydrogen phthalate) at pH 3 and pH 7, and (b) theoretical chemical oxygen demand (COD_{TH}) for any compound at Ti|NT-TiO_2 anode at pH 7.

Table 1
Chemical parameters of the organic compounds used for photoelectrocatalytic COD determination, along with acidity constants for the TiO_2 catalyst.

Substance	Molecular weight (g mol^{-1})	Ionization (acidity) constant (pK_a)	Reference
Hydrogen phthalate anion (HP^-)	204.22	HP^-/P^{2-} : 5.40	[47]
Glucose (G)	180.156	G/G^- : 12.18 G^-/G^{2-} : 13.90	[48] [49]
Acetic acid (AA, HAc)	60.05	HAc/Ac^- : 4.75	[50]
Aspirin (Acetylsalicylic acid, ASA)	180.16	ASA/ASA^- : 3.50	[51]
Terasil Blue dye (TB)	349.13	TB/TB^- : 5.68	[52]
TiO_2 catalyst: $TiOH_2^+/TiOH$ ($pK_{a_1} = 5.4$); $TiOH/TiO^-$ ($pK_{a_2} = 7.6$)			

that all target compounds follow a linear relationship between Δq and COD_{TH}. The data of Fig. 4b were fitted very well with the following linear equation: $\Delta q = 1.4857 \times 10^{-5} COD_{TH}$, with a correlation coefficient $R^2 = 0.9942$. Therefore, the photoelectrocatalytic quantification of chemical oxygen demand (COD_{PEC}) of organic matter can be made using this linear equation as calibration curve: $COD_{PEC} = \Delta q/1.4857 \times 10^{-5}$. This linear correlation was used to determine the COD_{PEC} of two organic compounds: ASA, purchased at a local pharmacy, and TB from a local textile. These compounds were photoelectrocatalytically oxidized under similar conditions in water with 50 mM Na_2SO_4 at pH 7, employing different concentrations of ASA (1, 2, 4 and 5 mg L^{-1}) and TB (3.6, 7.2, 10.8 and 14.4 mg L^{-1}). At each concentration tested in triplicate, the Δq value was obtained from the recorded photocurrent transients at the Ti|NT-TiO_2 anode. Then, the COD_{PEC} values for ASA and TB were calculated using the linear correlation above mentioned. Fig. 5a shows a plot of the COD_{PEC} values, for all tested organic compounds (KHP, G, AA, ASA and TB), against their theoretical COD (COD_{TH}) values. A linear relationship is observed between both parameters, showing a slope close to one (1.0469) for the best linear fit, with a correlation coefficient $R^2 =$ 0.9931 that corroborates the very good agreement between the data. Such behavior confirms that the recorded photocurrents are independent of the compound structure when they are photoelectrocatalytically oxidized under analogous conditions. These results show that COD can be reliably detected by the photoelectrocatalytic method using the Ti|NT-TiO_2 photoanode. In addition, a plot of COD_{PEC} versus the concentration of KHP, G, AA, ASA and TB shows a proportional increase with

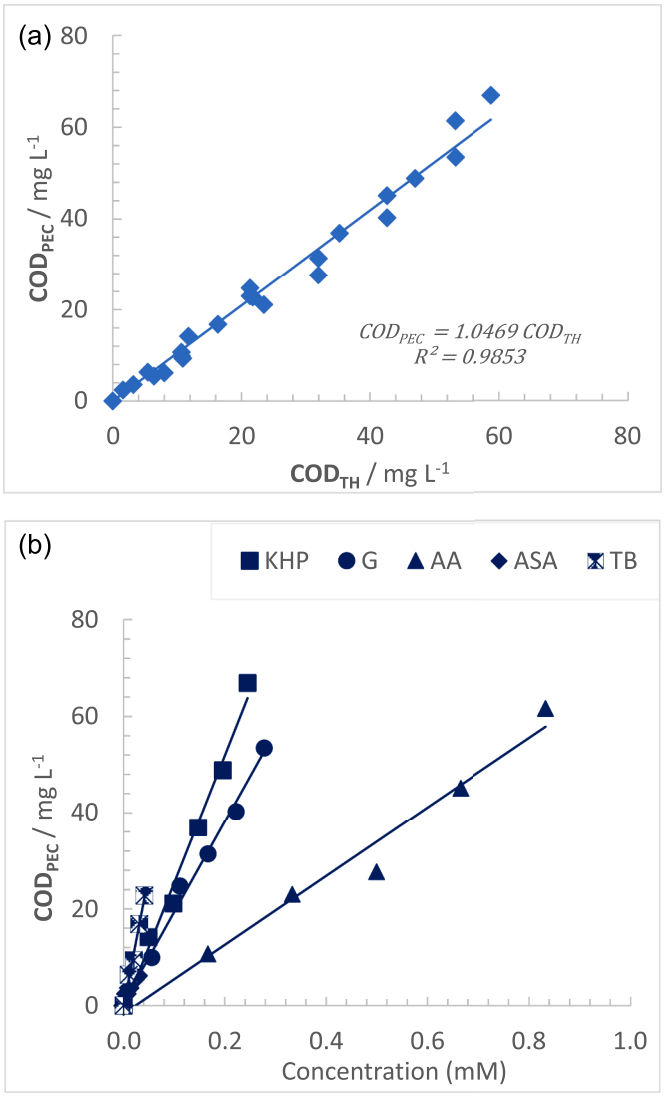

Fig. 5. Relationship between COD values (KHP, G, AA, ASA and TB) determined by photoelectrocatalysis and: (a) theoretical COD values with Ti|NT-TiO_2 electrode at pH 7, (b) concentration of organics.

the molecular weight of each organic compound, as depicted in Fig. 5b. Steeper curve slopes are obtained as the molar mass of the compound becomes higher, which is again consistent with the larger number of electrons involved when comparing reactions (3) to (1) (i.e., from 8 to 30 electrons), as well as (4) to (5) (28 and 66 electrons, respectively) for the photoelectrocatalytic degradation of the organic compounds.

$$\text{ASA}: \ C_7H_6O_3 + 11H_2O \rightarrow 7CO_2 + 28H^+ + 28e^- \quad (4)$$

$$\text{TB}: \ C_{14}H_9BrN_2O_4 + 30H_2O \rightarrow 14CO_2 + Br^- + 2NO_3^- + 69H^+ + 66e^- \quad (5)$$

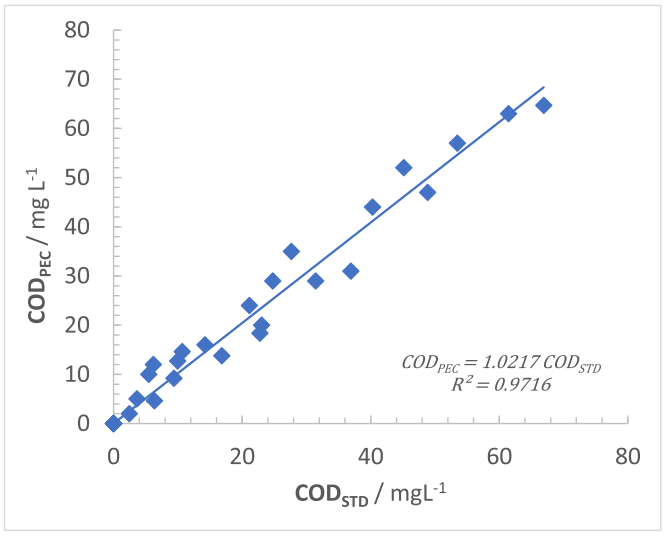

Fig. 6. Relationship between COD values determined for KHP, G, AA, ASA and TB by photoelectrocatalysis with Ti|NT-TiO_2 electrode at pH 7 and COD values analyzed by the standard method.

Fig. 6 shows a comparison between the standard chemical oxygen demand (COD_{STD}) analysis for all the target compounds, including ASA and TB, obtained using standard reagents and the standard procedure, and the COD detected by the proposed photoelectrocatalytic method. A good linear correlation was obtained, with a slope of 1.0217 and R^2 = 0.9871, showing good agreement with the standard method. These results validate the proposed method for COD analysis, since they demonstrate the validity of the PEC technique regardless of the analyte studied. Furthermore, a descriptive statistics method, known as box plot [46], has been applied to compare the distribution of the COD_{PEC} and COD_{STD} data sets, as shown in Fig. 7. It can be seen that COD_{PEC} and COD_{STD} present left-skewed data, so the data may not be normally distributed. However, there are no outliers. The COD_{PEC} data showed greater dispersion than the COD_{STD}. The median value of COD_{PEC} is slightly higher than that of COD_{STD}.

The limit of detection (LOD) of the photoelectrocatalytic method was calculated using the following equation: LOD = $\frac{3.3\ SE}{S}$, where SE is the standard deviation of the y-intercept of the regression curve, and S is the slope value of the linear best fitting of the correlation between Δq and COD_{TH}. This resulted in LOD = 3.6 mg L^{-1} for the developed photoelectrocatalytic method. This method can be applied at concentrations of organic pollutants between 0-50 mg L^{-1}, where its response is linear. In addition, Table 2 shows a comparison between the experimental and statistical parameters reported in the literature with the results obtained in the present work. It can be observed that the implemented methodology has a competitive performance, and in some cases is even superior, since the validation carried out using statistical parameters is within the reported intervals despite having diverse experimental variables. Regarding the LOD, this work has the second lowest value and hence, this analytical methodology is reliable for the detection of COD at low concentrations.

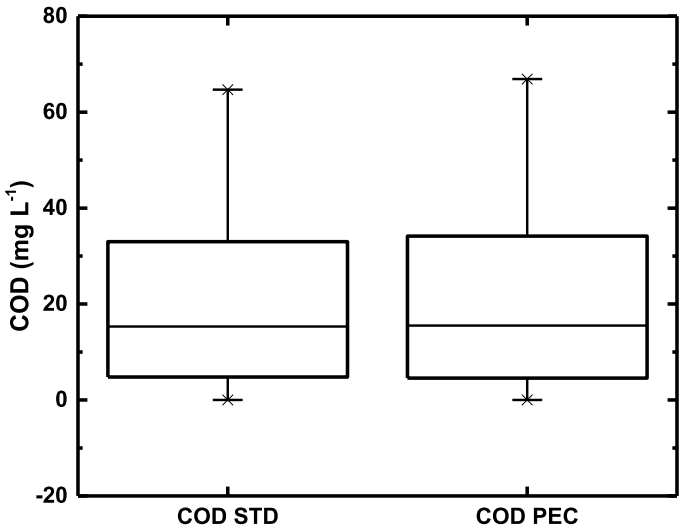

Fig. 7. Comparative box plot results between COD values determined for all model compounds by photoelectrocatalysis with Ti|NT-TiO_2 electrode at pH 7 and standard method.

Table 2
Comparative results of COD_{PEC} determination under UV light.

Reference	Electrode	Chemical compounds analyzed[a]	Electrolyte	Linear correlation (R^2 or R)	LOD (mg L^{-1})
[35]	ITO-TiO_2	KHP, GGA and OECD Real samples	2 mol L^{-1} $NaNO_3$	y=0.9987x - 0.3932; R = 0.995 y= 1.004x - 0.0384; R = 0.987	0.2
[3]	Ti|NT-TiO_2 reduced	KHP, G, LA, PH, AA	0.1 mol L^{-1} Na_2SO_4, pH 7.9	y=0.9989x; R^2 = 0.9928	8
[53]	Ti|NT-TiO_2	KHP	0.1 mol L^{-1} Na_2SO_4, pH 8	y= 1.0095x; R= 0.9895	16
[32]	CuO_2-TNTAs	KPH, G, GL, S, and LA	0.1 mol L^{-1} Na_2SO_4	y= 0.997x - 0.418; R^2 = 0.9873	15
[34]	Rutile TiO_2 nanorod arrays	KPH, G, GL, S, and LA	0.1 mol L^{-1} Na_2SO_4, pH 7	y = 0.9339x + 5.7058; R = 0.9901	18.3
[31]	NT-TiO_2	G, KHP, OA, GA and NAReal samples, mixtures	0.1 mol L^{-1} $NaHPO_4$	y = (0.000187 ± 0.0000027)x – (0.010240 ± 0.00125); R^2 = 0.9872	13
[10]	NT-TiO_2	An, RhB, KHP	0.1 mol L^{-1} Na_2SO_4	y = 0.59x + 14.31; R^2 = 0.991 y = 0.53x + 11.50; R^2 = 0.996 y = 0.49x + 7.90; R^2 = 0.996	5
[30]	NT-TiO_2	G, KHP, GA, AC,	NaH_2PO_4	y = 0.01142x+7.3606 × 10^{-5}; R^2 = 0.9959	-
[54]	Sulfurized NT-TiO_2	R120, R140, B160	0.1 mol L^{-1} $NaNO_3$	-	-
This work	Ti|NT-TiO_2 reduced	KHP, G, AA, ASA and TB	0.05 mol L^{-1} Na_2SO_4, pH 7	y = 1.0217x; R^2 = 0.9871	3.6

[a] Organic compounds analyzed: Acetic acid (AA), acetone (AC), acetyl salicylic acid (ASA), aniline (An), glycine (GL), glucose (G), glucose + glutamic acid (GGA), glutamic acid (GA), lactic acid (LA), nicotinic acid (NA), oxalic acid (OA), peptone + beef extract + urea (OECD), phenol (PH), potassium hydrogen phthalate (KHP), Reactive Blue 160 (B160), Reactive Red 120 (R120), Reactive Red 140 (R140), Rhodamine B (RhB), sucrose (S).

4. Conclusions

The main advantages of the electrochemical determination of solution COD by the photoelectrocatalytic method are the simplicity of the Ti|NT-TiO_2 photoanode synthesis methodology, the simplicity and short analysis time of the photoelectrocatalytic method, and the non-toxicity due to the absence of hazardous reagents. The photoelectrocatalytic method using the Ti|NT-TiO_2 photoanode under UV light represents a simple, economical and environmentally-friendly alternative to the standard method for measuring water quality.

The COD values obtained by the photoelectrocatalytic method were comparable with those from the standard method. This method was successfully applied to determine COD for different initial concentrations of two commonly used compounds, such as aspirin and Terasil Blue dye, yielding good results compared to the standard method. The proposed method shows an LOD of 3.6 mg L^{-1} and linearity within the concentration range of 0-50 mg L^{-1}, as has been verified for hydrogen phthalate, glucose and acetic acid as model compounds.

CRediT authorship contribution statement

Patricia García-Ramírez: Data curation, Investigation, Methodology. **Carlos Antonio Pineda-Arellano:** Investigation, Methodology. **Daysi Elusaí Millán-Ocampo:** Investigation, Methodology. **Alberto Álvarez-Gallegos:** Data curation, Funding acquisition. **Ignasi Sirés:** Data curation, Funding acquisition, Validation, Writing – original draft, Writing – review & editing. **Susana Silva-Martínez:** Conceptualization, Data curation, Funding acquisition, Project administration, Resources, Supervision, Validation, Writing – original draft, Writing – review & editing.

Declaration of Competing Interest

The authors declare that they have no known competing financial interests or personal relationships that could have appeared to influence the work reported in this paper.

Data availability

Data will be made available on request.

Acknowledgments

I.S. gratefully acknowledge financial support from projects PID2019-109291RB-I00 and PID2022-140378OB-I00 (MCIN/AEI/10.13039/501100011033, Spain, co-funded by the EU).

References

[1] P. Namour, N. Jaffrezic-Renault, P. Namour, Sensors for measuring biodegradable and total organic matter in water, TrAC - Trends Anal. Chem. 29 (2010) 848–857, https://doi.org/10.1016/j.trac.2010.04.013.
[2] X. Chen, L. Peng, J. Wang, D. Zhang, Y. Zhao, Q. Zhao, T. Li, Determination of chemical oxygen demand in water samples using gas-phase molecular absorption spectrometry, Anal. Sci. 36 (2020) 841–846, https://doi.org/10.2116/analsci.19P444.
[3] Z. Zhang, X. Chang, A. Chen, Determination of chemical oxygen demand based on photoelectrocatalysis of nanoporous TiO_2 electrodes, Sensors Actuators B: Chem 223 (2016) 664–670, https://doi.org/10.1016/j.snb.2015.10.001.
[4] S. Jouanneau, L. Recoules, M.J. Durand, A. Boukabache, V. Picot, Y. Primault, A. Lakel, M. Sengelin, B. Barillon, G. Thouand, Methods for assessing biochemical oxygen demand (BOD): a review, Water Res 49 (2014) 62–82, https://doi.org/10.1016/j.watres.2013.10.066.
[5] T. Kondo, Y. Tamura, M. Hoshino, T. Watanabe, T. Aikawa, M. Yuasa, Y. Einaga, Direct determination of chemical oxygen demand by anodic decomposition of organic compounds at a diamond electrode, Anal. Chem. 86 (2014) 8066–8072, https://doi.org/10.1021/ac500919k.
[6] B.A. Schumacher, Methods for the Determination of Total Organic Carbon (TOC) in Soils and Sediments (2002), Environmental Protection Agency, Washington DC.
[7] J. Ma, Determination of chemical oxygen demand in aqueous samples with non-electrochemical methods, Trends Environ. Anal. Chem. 14 (2017) 37–43, https://doi.org/10.1016/j.teac.2017.05.002.
[8] Y. Ge, Y. Zhai, D. Niu, Y. Wang, C. Fernandez, T. Ramakrishnappa, X. Hu, L. Wang, Electrochemical determination of chemical oxygen demand using Ti/TiO_2 electrode, Int. J. Electrochem. Sci. 11 (2016) 9812–9821, https://doi.org/10.20964/2016.12.05.
[9] M. Gutiérrez-Capitán, A. Baldi, R. Gómez, V. García, C. Jiménez-Jorquera, C. Fernández-Sánchez, Electrochemical nanocomposite-derived sensor for the analysis of chemical oxygen demand in urban wastewaters, Anal. Chem. 87 (2015) 2152–2160, https://doi.org/10.1021/ac503329a.
[10] X. Li, L. Wang, L. Wang, Determination of chemical oxygen demand in mixed organic solution by Ti/TiO_2 nanotube array electrode method, Water Sci. Technol. 84 (2021) 865–879, https://doi.org/10.2166/wst.2021.284.
[11] H. Si, X. Zhang, S. Lin, A simple flow injection sensing system for the real-time on-line determination of chemical oxygen demand based on 3D Au-NPs/TiO_2 nanotube arrays, Front. Mater. 6 (2019) 1–7, https://doi.org/10.3389/fmats.2019.00238.
[12] H. Kabir, H. Zhu, R. Lopez, N.W. Nicholas, D.N. McIlroy, E. Echeverria, J. May, I. F. Cheng, Electrochemical determination of chemical oxygen demand on functionalized pseudo-graphite electrode, J. Electroanal. Chem. 851 (2019), 113448, https://doi.org/10.1016/j.jelechem.2019.113448.
[13] H. Yu, H. Wang, X. Quan, S. Chen, Y. Zhang, Amperometric determination of chemical oxygen demand using boron-doped diamond (BDD) sensor, Electrochem. Commun. 9 (2007) 2280–2285, https://doi.org/10.1016/j.elecom.2007.06.037.
[14] R. Bogdanowicz, J. Czupryniak, M. Gnyba, J. Ryl, T. Ossowski, M. Sobaszek, K. Darowicki, Determination of chemical oxygen demand (COD) at borondoped diamond (BDD) sensor by means of amperometric technique, Procedia Eng 47 (2012) 1117–1120, https://doi.org/10.1016/j.proeng.2012.09.347.
[15] J. Wang, C. Wu, K. Wu, Q. Cheng, Y. Zhou, Electrochemical sensing chemical oxygen demand based on the catalytic activity of cobalt oxide film, Anal. Chim. Acta. 736 (2012) 55–61, https://doi.org/10.1016/j.aca.2012.05.046.
[16] H.H. Hassan, I.H.A. Badr, H.T.M. Abdel-Fatah, E.M.S. Elfeky, A.M. Abdel-Aziz, Low cost chemical oxygen demand sensor based on electrodeposited nano-copper film, Arab. J. Chem. 11 (2018) 171–180, https://doi.org/10.1016/j.arabjc.2015.07.001.
[17] T. Jing, Y. Zhou, Q. Hao, Y. Zhou, S. Mei, A nano-nickel electrochemical sensor for sensitive determination of chemical oxygen demand, Anal. Methods. 4 (2012) 1155–1159, https://doi.org/10.1039/c2ay05631c.
[18] Q. Zhou, X. Zhou, R. Zheng, Z. Liu, J. Wang, Application of lead oxide electrodes in wastewater treatment: a review, Sci. Total Environ. 806 (2022), 150088, https://doi.org/10.1016/j.scitotenv.2021.150088.
[19] X. Li, Y. Shang, C. Fernandez, T. Pei, L. Wang, Electrochemical determination of chemical oxygen demand in mixed organic solution by Al/SnO_2-TiO_2 electrode, Int. J. Electrochem. Sci. 16 (2021) 1–20, https://doi.org/10.20964/2021.11.45.
[20] D. Jiang, H. Zhao, S. Zhang, R. John, Characterization of photoelectrocatalytic processes at nanoporous TiO_2 film electrodes: photocatalytic oxidation of glucose, J. Phys. Chem. B. 107 (2003) 12774–12780, https://doi.org/10.1021/jp0307349.
[21] H. Atout, M.G. Álvarez, D. Chebli, A. Bouguettoucha, D. Tichit, J. Llorca, F. Medina, Enhanced photocatalytic degradation of methylene blue: preparation of TiO_2/reduced graphene oxide nanocomposites by direct sol-gel and hydrothermal methods, Mater. Res. Bull. 95 (2017) 578–587, https://doi.org/10.1016/j.materresbull.2017.08.029.
[22] Z. Cui, M. Zhao, X. Que, J. Wang, Y. Xu, M.N. Ghazzal, C. Colbeau-Justin, D. Pan, W. Wu, Facile vacuum annealing-induced modification of TiO_2 with an enhanced photocatalytic performance, ACS Omega 6 (2021) 27121–27128, https://doi.org/10.1021/acsomega.1c03762.
[23] L. Pan, S. Wang, J.J. Zou, Z.F. Huang, L. Wang, X. Zhang, Ti^{3+}-defected and V-doped TiO_2 quantum dots loaded on MCM-41, Chem. Commun. 50 (2014) 988–990, https://doi.org/10.1039/c3cc47752e.
[24] P. Sudhagar, A. Devadoss, T. Song, P. Lakshmipathiraj, H. Han, V.V. Lysak, C. Terashima, K. Nakata, A. Fujishima, U. Paik, Y.S. Kang, Enhanced photocatalytic performance at a Au/N-TiO_2 hollow nanowire array by a combination of light scattering and reduced recombination, Phys. Chem. Chem. Phys. 16 (2014) 17748–17755, https://doi.org/10.1039/c4cp02009j.
[25] Y. Duan, J. Zheng, M. Xu, X. Song, N. Fu, Y. Fang, X. Zhou, Y. Lin, F. Pan, Metal and F dual-doping to synchronously improve electron transport rate and lifetime for TiO_2 photoanode to enhance dye-sensitized solar cells performances, J. Mater. Chem. A. 3 (2015) 5692–5700, https://doi.org/10.1039/c4ta07068b.
[26] A. Thiam, I. Sirés, P.L. Cabot, F. Alcaide, Photodegradation of Methylene Blue using Nb-doped titania nanotubes with adsorption and photocatalytic properties, Mater. Lett. 338 (2023), https://doi.org/10.1016/j.matlet.2023.134024.
[27] R. Oriol, I. Sirés, E. Brillas, A.R. De Andrade, A hybrid photoelectrocatalytic/photoelectro-Fenton treatment of Indigo Carmine in acidic aqueous solution using TiO_2 nanotube arrays as photoanode, J. Electroanal. Chem. 847 (2019) 1–10, https://doi.org/10.1016/j.jelechem.2019.04.048.
[28] X. Chang, S.S. Thind, A. Chen, Electrocatalytic enhancement of salicylic acid oxidation at electrochemically reduced TiO_2 nanotubes, ACS Catal 4 (2014) 2616–2622, https://doi.org/10.1021/cs500487a.
[29] B. Bastug Azer, A. Gulsaran, J.R. Pennings, R. Saritas, S. Kocer, J.L. Bennett, Y. Devdas Abhang, M.A. Pope, E. Abdel-Rahman, M. Yavuz, A Review: tiO_2 based photoelectrocatalytic chemical oxygen demand sensors and their usage in industrial applications, J. Electroanal. Chem. 918 (2022), 116466, https://doi.org/10.1016/j.jelechem.2022.116466.
[30] Q. Zheng, B. Zhou, F. Bai, L. Li, Z. Jin, J. Zhang, J. Li, Y. Liu, W. Cai, X. Zhu, Self-organized TiO_2 nanotube array sensor for the determination of chemical oxygen demand, Adv. Mater. 20 (2008) 1044–1049, https://doi.org/10.1002/adma.200701619.
[31] J. Zhang, B. Zhou, Q. Zheng, J. Li, J. Bai, Y. Liu, W. Cai, Photoelectrocatalytic COD determination method using highly ordered TiO_2 nanotube array, Water Res 43 (2009) 1986–1992, https://doi.org/10.1016/j.watres.2009.01.035.
[32] C. Wang, J. Wu, P. Wang, Y. Ao, J. Hou, J. Qian, Photoelectrocatalytic determination of chemical oxygen demand under visible light using Cu_2O-loaded TiO_2 nanotube arrays electrode, Sensors Actuators B: Chem 181 (2013) 1–8, https://doi.org/10.1016/j.snb.2013.02.011.
[33] M. Nurdin, I. Ilham, M. Maulidiyah, M.Z. Muzakkar, D. Wibowo, Z. Arham, L.O. A. Salim, I. Irwan, C. Bijang, A.A. Umar, Enhanced photoelectrocatalytic performance using chalcogenide Te/TiO_2/Ti nanotube array based on COD analyses for water treatment applications, Electrocatalysis 14 (2023) 581–592, https://doi.org/10.1007/s12678-023-00820-3.
[34] C. Wang, J. Wu, W. Peifang, A. Yanhui, H. Jun, Q. Jin, Investigation on the application of titania nanorod arrays to the determination of chemical oxygen demand, Anal. Chim. Acta. 767 (2013) 141–147.
[35] H. Zhao, D. Jiang, S. Zhang, K. Catterall, R. John, Development of a direct photoelectrochemical method for determination of chemical oxygen demand, Anal. Chem. 76 (2004) 155–160, https://doi.org/10.1021/ac0302298.
[36] X. Chang, S.S. Thind, M. Tian, M.M. Hossain, A. Chen, Significant enhancement of the photoelectrochemical activity of nanoporous TiO_2 for environmental applications, Electrochim. Acta. 173 (2015) 728–735, https://doi.org/10.1016/j.electacta.2015.05.122.
[37] P. García-Ramírez, E. Ramírez-Morales, J.C. Cortazar, I. Sirés, S. Silva-Martínez, Influence of ruthenium doping on UV-and visible-light photoelectrocatalytic color removal from dye solutions using a TiO_2 nanotube array photoanode, Chemosphere 267 (2021), 128925, https://doi.org/10.1016/j.chemosphere.2020.128925.
[38] J. Georgieva, E. Valova, S. Armyanov, N. Philippidis, I. Poulios, S. Sotiropoulos, Bi-component semiconductor oxide photoanodes for the photoelectrocatalytic oxidation of organic solutes and vapours: a short review with emphasis to TiO_2-WO_3 photoanodes, J. Hazard. Mater. (2012) 30–46, https://doi.org/10.1016/j.jhazmat.2011.11.069, 211–212.
[39] P.S. Basavarajappa, S.B. Patil, N. Ganganagappa, K.R. Reddy, A.V. Raghu, C. V. Reddy, Recent progress in metal-doped TiO_2, non-metal doped/codoped TiO_2 and TiO_2 nanostructured hybrids for enhanced photocatalysis, Int. J. Hydrogen Energy. 45 (2020) 7764–7778, https://doi.org/10.1016/j.ijhydene.2019.07.241.
[40] K. Changanaqui, E. Brillas, H. Alarcón, I. Sirés, ZnO/TiO_2/Ag_2Se nanostructures as photoelectrocatalysts for the degradation of oxytetracycline in water, Electrochim. Acta. 331 (2020), 135194, https://doi.org/10.1016/j.electacta.2019.135194.

[41] Y. Wang, M. Zu, X. Zhou, H. Lin, F. Peng, S. Zhang, Designing efficient TiO_2-based photoelectrocatalysis systems for chemical engineering and sensing, Chem. Eng. J. 381 (2020), 122605, https://doi.org/10.1016/j.cej.2019.122605.
[42] M.R. Hoffmann, S.T. Martin, W. Choi, D.W. Bahnemann, Environmental applications of semiconductor photocatalysis, Chem. Rev. 95 (1995) 69–96, https://doi.org/10.1021/cr00033a004.
[43] P.R. Gogate, A.B. Pandit, Sonophotocatalytic reactors for wastewater treatment: a critical review, AIChE J 50 (2004) 1051–1079, https://doi.org/10.1002/aic.10079.
[44] T. Preocanin, N. Kallay, Point of zero charge and surface charge density of TiO_2 in aqueous electrolyte solution as obtained by potentiometric mass titration, Croat. Chem. Acta. 79 (2006) 95–106.
[45] E. Koumaki, D. Mamais, C. Noutsopoulos, M.C. Nika, A.A. Bletsou, N.S. Thomaidis, A. Eftaxias, G. Stratogianni, Degradation of emerging contaminants from water under natural sunlight: the effect of season, pH, humic acids and nitrate and identification of photodegradation by-products, Chemosphere 138 (2015) 675–681, https://doi.org/10.1016/j.chemosphere.2015.07.033.
[46] K. Potter, Methods for presenting statistical information: the Box Plot, Vis, Large Unstructured Data Sets 4 (2006) 97–106.
[47] D. Midgley, Determination of the stability constants of nitritoborate ion by means of an NO_x-selective electrode and of boric acid complexes of acetate and phthalate by pH measurement, J. Chem. Soc. Dalt. Trans. (1991) 1585–1588, https://doi.org/10.1039/DT9910001585.
[48] S. Malerz, K. Mudryk, L. Tomaník, D. Stemer, U. Hergenhahn, T. Buttersack, F. Trinter, R. Seidel, W. Quevedo, C. Goy, I. Wilkinson, S. Thürmer, P. Slavíček, B. Winter, Following in Emil Fischer's Footsteps: a site-selective probe of glucose acid-base chemistry, J. Phys. Chem. A. 125 (2021) 6881–6892, https://doi.org/10.1021/acs.jpca.1c04695.
[49] P.A. Shaffer, T.E. Friedemann, Sugar activation by alkali, J. Biol. Chem. 86 (1930) 345–374, https://doi.org/10.1016/s0021-9258(18)76931-7.
[50] R. Cao, X. Liu, J. Guo, Y. Xu, Comparison of various organic acids for xylo-oligosaccharide productions in terms of pK_a values and combined severity, Biotechnol. Biofuels 14 (2021) 1–9, https://doi.org/10.1186/s13068-021-01919-9.
[51] H. Raabová, J. Erben, J. Chvojka, P. Solich, F. Švec, D. Šatínský, The role of pK_a, log P of analytes, and protein matrix in solid-phase extraction using native and coated nanofibrous and microfibrous polymers prepared via meltblowing and combined meltblowing/electrospinning technologies, Talanta 232 (2021), https://doi.org/10.1016/j.talanta.2021.122470.
[52] Guidechem Directory, 2022. Terasil Blue dye chemical information. https://www.guidechem.com/encyclopedia/1-5-diaminobromo-4-8-dihydroxy-dic191881.html#1.2 (Accessed September 27, 2023).
[53] J. Li, L. Zheng, L. Li, G. Shi, Y. Xian, L. Jin, Ti/TiO_2 electrode preparation using laser anneal and its application to determination of chemical oxygen demand, Electroanalysis 18 (2006) 1014–1018, https://doi.org/10.1002/elan.200503481.
[54] M. Nurdin, M.Z. Muzakkar, T. Trisna, Z. Arham, L.O.A. Salim, I. Irwan, A.A. Umar, High performance COD detection of organic compounds pollutants using sulfurized-TiO_2/Ti nanotubes arrays photoelectrocatalyst, Electrocatalysis 13 (2022) 580–589.